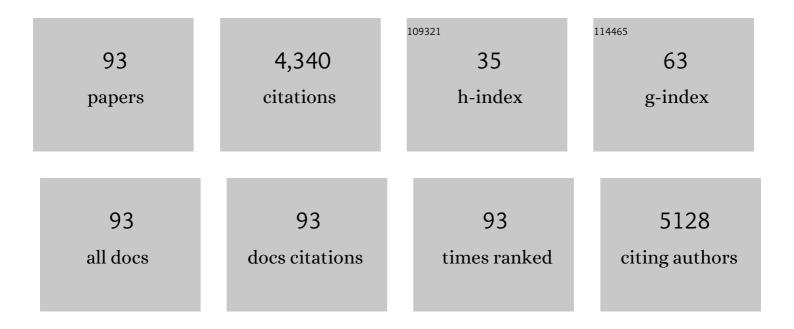
List of Publications by Year in descending order

Source: https://exaly.com/author-pdf/2362353/publications.pdf Version: 2024-02-01



#	Article	IF	CITATIONS
1	Photo-induced enhancement of lattice fluctuations in metal-halide perovskites. Nature Communications, 2022, 13, 1019.	12.8	5
2	Unleashing the Full Power of Perovskite/Silicon Tandem Modules with Solar Trackers. ACS Energy Letters, 2022, 7, 1604-1610.	17.4	18
3	Damp heat–stable perovskite solar cells with tailored-dimensionality 2D/3D heterojunctions. Science, 2022, 376, 73-77.	12.6	366
4	Probing Ultrafast Interfacial Carrier Dynamics in Metal Halide Perovskite Films and Devices by Transient Reflection Spectroscopy. ACS Applied Materials & Interfaces, 2022, 14, 34281-34290.	8.0	5
5	Photoactivated p-Doping of Organic Interlayer Enables Efficient Perovskite/Silicon Tandem Solar Cells. ACS Energy Letters, 2022, 7, 1987-1993.	17.4	14
6	Study on the Performance of Oxygen-Rich Zn(O,S) Buffers Fabricated by Sputtering Deposition and Zn(O,S)/Cu(In,Ga)(S,Se) ₂ Interfaces. ACS Applied Materials & Interfaces, 2022, 14, 24435-24446.	8.0	2
7	Monolithic Perovskite/Silicon Tandem Photovoltaics with Minimized Cell-to-Module Losses by Refractive-Index Engineering. ACS Energy Letters, 2022, 7, 2370-2372.	17.4	20
8	Efficient and stable perovskite-silicon tandem solar cells through contact displacement by MgF <i>_x </i> . Science, 2022, 377, 302-306.	12.6	141
9	Smooth and highly-crystalline Ag-doped CIGS films sputtered from quaternary ceramic targets. Ceramics International, 2021, 47, 2288-2293.	4.8	8
10	Scaling-up perovskite solar cells on hydrophobic surfaces. Nano Energy, 2021, 81, 105633.	16.0	46
11	Efficient bifacial monolithic perovskite/silicon tandem solar cells via bandgap engineering. Nature Energy, 2021, 6, 167-175.	39.5	164
12	Potassium Thiocyanateâ€Assisted Enhancement of Slotâ€Dieâ€Coated Perovskite Films for Highâ€Performance Solar Cells. Small Science, 2021, 1, 2000044.	9.9	26
13	Tin Oxide Electronâ€5elective Layers for Efficient, Stable, and Scalable Perovskite Solar Cells. Advanced Materials, 2021, 33, e2005504.	21.0	196
14	Potassium Thiocyanateâ€Assisted Enhancement of Slotâ€Dieâ€Coated Perovskite Films for Highâ€Performance Solar Cells. Small Science, 2021, 1, 2170013.	9.9	9
15	Concurrent cationic and anionic perovskite defect passivation enables 27.4% perovskite/silicon tandems with suppression of halide segregation. Joule, 2021, 5, 1566-1586.	24.0	119
16	Toward Stable Monolithic Perovskite/Silicon Tandem Photovoltaics: A Six-Month Outdoor Performance Study in a Hot and Humid Climate. ACS Energy Letters, 2021, 6, 2944-2951.	17.4	42
17	Linked Nickel Oxide/Perovskite Interface Passivation for Highâ€Performance Textured Monolithic Tandem Solar Cells. Advanced Energy Materials, 2021, 11, 2101662.	19.5	77
18	Ligand-bridged charge extraction and enhanced quantum efficiency enable efficient n–i–p perovskite/silicon tandem solar cells. Energy and Environmental Science, 2021, 14, 4377-4390.	30.8	79

#	Article	IF	CITATIONS
19	Linked Nickel Oxide/Perovskite Interface Passivation for Highâ€Performance Textured Monolithic Tandem Solar Cells (Adv. Energy Mater. 40/2021). Advanced Energy Materials, 2021, 11, 2170160.	19.5	2
20	28.2%-efficient, outdoor-stable perovskite/silicon tandem solar cell. Joule, 2021, 5, 3169-3186.	24.0	99
21	Reduced mineral fertilization coupled with straw return in field mesocosm vegetable cultivation helps to coordinate greenhouse gas emissions and vegetable production. Journal of Soils and Sediments, 2020, 20, 1834-1845.	3.0	23
22	Gamma-ray irradiation-induced oxidation and disproportionation at the amorphous SiO ₂ /Si interfaces. Journal of Materials Chemistry C, 2020, 8, 17065-17073.	5.5	5
23	Mixedâ€Cation MA _{<i>x</i>} Cs _{1â^'<i>x</i>} PbBr ₃ Perovskite Single Crystals with Composition Management for Highâ€Sensitivity Xâ€Ray Detection. Physica Status Solidi - Rapid Research Letters, 2020, 14, 2000226.	2.4	14
24	High-Performance Perovskite Single-Junction and Textured Perovskite/Silicon Tandem Solar Cells via Slot-Die-Coating. ACS Energy Letters, 2020, 5, 3034-3040.	17.4	134
25	Optimization of CulnGaSSe properties and CulnGaSSe/CdS interface quality for efficient solar cells processed with CulnGa precursors. Journal of Power Sources, 2020, 479, 229105.	7.8	8
26	Lewis-Acid Doping of Triphenylamine-Based Hole Transport Materials Improves the Performance and Stability of Perovskite Solar Cells. ACS Applied Materials & Interfaces, 2020, 12, 23874-23884.	8.0	38
27	Defect Passivation in Perovskite Solar Cells by Cyanoâ€Based Ï€â€Conjugated Molecules for Improved Performance and Stability. Advanced Functional Materials, 2020, 30, 2002861.	14.9	87
28	Nitrous oxide emission and the related denitrifier community: A short-term response to organic manure substituting chemical fertilizer. Ecotoxicology and Environmental Safety, 2020, 192, 110291.	6.0	25
29	Partial substitution of chemical fertilizer by organic materials changed the abundance, diversity, and activity of nirS-type denitrifying bacterial communities in a vegetable soil. Applied Soil Ecology, 2020, 152, 103589.	4.3	25
30	Solutionâ€Processed MAPbBr ₃ and CsPbBr ₃ Singleâ€Crystal Detectors with Improved Xâ€Ray Sensitivity via Interfacial Engineering. Physica Status Solidi (A) Applications and Materials Science, 2020, 217, 2000104.	1.8	24
31	Polysilicon Passivating Contacts for Silicon Solar Cells: Interface Passivation and Carrier Transport Mechanism. ACS Applied Energy Materials, 2019, 2, 4609-4617.	5.1	41
32	The effects of preheating temperature on CuInGaSe2/CdS interface and the device performances. Solar Energy, 2019, 194, 11-17.	6.1	13
33	Effects of Different Soil Amendments Application on Soil Aggregate Stability and Soil Consistency under Wetting and Drying Altered Planting System. Communications in Soil Science and Plant Analysis, 2019, 50, 2263-2277.	1.4	5
34	A Review of the Role of Solvents in Formation of High-Quality Solution-Processed Perovskite Films. ACS Applied Materials & Interfaces, 2019, 11, 7639-7654.	8.0	113
35	Triarylphosphine Oxide as Cathode Interfacial Material for Inverted Perovskite Solar Cells. Advanced Materials Interfaces, 2019, 6, 1900434.	3.7	16
36	Influences of Ga concentration on performances of CuInGaSe2 cells fabricated by sputtering-based method with ceramic quaternary target. Ceramics International, 2019, 45, 16405-16410.	4.8	11

#	Article	IF	CITATIONS
37	Variation in N2O emission and N2O related microbial functional genes in straw- and biochar-amended and non-amended soils. Applied Soil Ecology, 2019, 137, 57-68.	4.3	65
38	Tuning Bandgap of Mixedâ€Halide Perovskite for Improved Photovoltaic Performance Under Monochromaticâ€Light Illumination. Physica Status Solidi (A) Applications and Materials Science, 2019, 216, 1800727.	1.8	8
39	The effects of annealing temperature on CICSeS solar cells by sputtering from quaternary target with H2S post annealing. Applied Surface Science, 2019, 473, 848-854.	6.1	8
40	10.3%-efficient submicron-thick Cu(In,Ga)Se2 solar cells with absorber fabricated by sputtering In2Se3, CuGaSe2 and Cu2Se targets. Applied Surface Science, 2018, 442, 308-312.	6.1	7
41	An investigation on performance enhancement for KF post deposition treated CIGS solar cells fabricated by sputtering CIGS quaternary targets. Vacuum, 2018, 151, 233-236.	3.5	13
42	Ga2Se3 treatment of Cu-rich CIGS thin films to fabricate Cu-poor CIGS thin films with large grains and U-shaped Ga distribution. Vacuum, 2018, 152, 184-187.	3.5	8
43	Two-stage method to enhance the grain size of Cu(In,Ga)Se2 absorbers based on sputtering quaternary Cu(In,Ga)Se2 target. Materials Letters, 2018, 212, 165-167.	2.6	6
44	Study on how the content of selenium in the precursors influences the properties of CuInSe2 thin films. Applied Surface Science, 2018, 434, 452-455.	6.1	3
45	Copper Incorporation in Organicâ€Inorganic Hybrid Halide Perovskite Solar Cells. ChemistrySelect, 2018, 3, 12198-12204.	1.5	16
46	A 16.5% Efficient Perovskite Solar Cells With Inorganic NiO Film as Hole Transport Material. IEEE Journal of Photovoltaics, 2018, 8, 1039-1043.	2.5	17
47	Responses of soil carbon pool and soil aggregates associated organic carbon to straw and straw-derived biochar addition in a dryland cropping mesocosm system. Agriculture, Ecosystems and Environment, 2018, 265, 576-586.	5.3	115
48	Fabrication of wide band-gap CuGaSe2 solar cells for tandem device applications by sputtering from a ternary target and post selenization treatment. Materials Letters, 2018, 230, 128-131.	2.6	8
49	Pre-deposition of CdS layers to improve the diode quality of CZTSSe solar cells. Materials Letters, 2018, 229, 372-374.	2.6	3
50	Multi-layer strategy to enhance the grain size of CIGS thin film fabricating by single quaternary CIGS target. Journal of Alloys and Compounds, 2017, 710, 172-176.	5.5	19
51	FAPb _{1â^²x} Sn _x I ₃ mixed metal halide perovskites with improved light harvesting and stability for efficient planar heterojunction solar cells. Journal of Materials Chemistry A, 2017, 5, 9097-9106.	10.3	56
52	Eliminating the excess Cu x Se phase in Cu-rich Cu(In,Ga)Se 2 by In 2 Se 3 treatment. Journal of Alloys and Compounds, 2017, 709, 31-35.	5.5	9
53	Highly efficient random terpolymers for photovoltaic applications with enhanced absorption and molecular aggregation. Chinese Journal of Polymer Science (English Edition), 2017, 35, 249-260.	3.8	21
54	Understanding the Role of the Electronâ€Transport Layer in Highly Efficient Planar Perovskite Solar Cells. ChemPhysChem, 2017, 18, 617-625.	2.1	44

#	Article	IF	CITATIONS
55	Fermi level alignment by copper doping for efficient ITO/perovskite junction solar cells. Journal of Materials Chemistry A, 2017, 5, 25211-25219.	10.3	53
56	Investigation on Sb-doped induced Cu(InGa)Se2 films grain growth by sputtering process with Se-free annealing. Solar Energy, 2017, 157, 1074-1081.	6.1	9
57	Soil aggregate and organic carbon distribution at dry land soil and paddy soil: the role of different straws returning. Environmental Science and Pollution Research, 2017, 24, 27942-27952.	5.3	76
58	Fabricating Cu(In,Ga)Se2 (CIGS) thin films with large grains based on the quaternary CIGS targets. Vacuum, 2017, 146, 282-286.	3.5	6
59	Understanding the Photovoltaic Performance of Perovskite–Spirobifluorene Solar Cells. ChemPhysChem, 2017, 18, 3030-3038.	2.1	12
60	A study on mechanisms of Sb-doping induced grain growth for Cu(InGa)Se2 absorbers deposited from quaternary targets. Journal of Alloys and Compounds, 2017, 727, 572-578.	5.5	4
61	Effects of Soil Conditioners on Aggregate Stability in a Clay Loam Soil: A Comparison Study of Biomass Ash with Other Four Conditioners. Communications in Soil Science and Plant Analysis, 2017, 48, 2294-2313.	1.4	5
62	Large band-gap copolymers based on a 1,2,5,6-naphthalenediimide unit for polymer solar cells with high open circuit voltages and power conversion efficiencies. Journal of Materials Chemistry A, 2016, 4, 7372-7381.	10.3	25
63	Solution-Processable Small Molecules for High-Performance Organic Solar Cells with Rigidly Fluorinated 2,2′-Bithiophene Central Cores. ACS Applied Materials & Interfaces, 2016, 8, 11639-11648.	8.0	46
64	Cu(In,Ga)Se2 solar cells fabricated by sputtering from copper-poor and selenium-rich ceramic target with selenium-free post treatment. Materials Letters, 2016, 184, 69-72.	2.6	7
65	Structures and Electronic Properties of Different CH3NH3PbI3/TiO2 Interface: A First-Principles Study. Scientific Reports, 2016, 6, 20131.	3.3	69
66	The role of Na incorporation in the low-temperature processed CIGS thin film solar cells using post deposition treatment. Journal of Alloys and Compounds, 2016, 658, 12-18.	5.5	25
67	Growth and evolution of solution-processed CH3NH3PbI3-xClx layer for highly efficient planar-heterojunction perovskite solar cells. Journal of Power Sources, 2016, 301, 242-250.	7.8	39
68	Locking the morphology with a green, fast and efficient physical cross-linking approach for organic electronic applications. Organic Electronics, 2016, 28, 53-58.	2.6	4
69	Formation of organic–inorganic mixed halide perovskite films by thermal evaporation of PbCl ₂ and CH ₃ NH ₃ I compounds. RSC Advances, 2015, 5, 26175-26180.	3.6	47
70	Influences of Na on sintering of Cu(In,Ga)Se2 quaternary ceramic targets. Journal of Alloys and Compounds, 2015, 636, 335-340.	5.5	12
71	Uncovering the Veil of the Degradation in Perovskite CH ₃ NH ₃ PbI ₃ upon Humidity Exposure: A First-Principles Study. Journal of Physical Chemistry Letters, 2015, 6, 3289-3295.	4.6	171
72	Annealing treatment of Cu(In,Ga)Se2 absorbers prepared by sputtering a quaternary target for 13.5% conversion efficiency device. Solar Energy, 2015, 118, 375-383.	6.1	24

#	Article	IF	CITATIONS
73	Low-temperature, solution processed metal sulfide as an electron transport layer for efficient planar perovskite solar cells. Journal of Materials Chemistry A, 2015, 3, 11750-11755.	10.3	122
74	Cu(In,Ga)Se ₂ solar cell with 16.7% active-area efficiency achieved by sputtering from a quaternary target. Physica Status Solidi (A) Applications and Materials Science, 2015, 212, 1774-1778.	1.8	38
75	Surface evolution of sputtered Cu(In,Ga)Se2 thin films under various annealing temperatures. Journal of Materials Science: Materials in Electronics, 2015, 26, 4840-4847.	2.2	10
76	Fabrication of Se-rich Cu(In1-XGaX)Se2 quaternary ceramic target. Vacuum, 2015, 119, 15-18.	3.5	11
77	Improved Crystallization of Perovskite Films by Optimized Solvent Annealing for High Efficiency Solar Cell. ACS Applied Materials & Interfaces, 2015, 7, 24008-24015.	8.0	257
78	Study on the performance of Tungsten–Titanium alloy film as a diffusion barrier for iron in a flexible CIGS solar cell. Solar Energy, 2015, 120, 357-362.	6.1	7
79	The relationships between electronic properties and microstructure of Cu(In,Ga)Se2 films prepared by sputtering from a quaternary target. Materials Letters, 2014, 137, 249-251.	2.6	18
80	Earth-abundant and low-cost CZTS solar cell on flexible molybdenum foil. RSC Advances, 2014, 4, 23666-23669.	3.6	54
81	Electrodeposited CZTS solar cells from Reline electrolyte. Green Chemistry, 2014, 16, 3841-3845.	9.0	54
82	Raman and XPS studies of CIGS/Mo interfaces under various annealing temperatures. Materials Letters, 2014, 136, 278-281.	2.6	23
83	Highly efficient fullerene/perovskite planar heterojunction solar cells via cathode modification with an amino-functionalized polymer interlayer. Journal of Materials Chemistry A, 2014, 2, 19598-19603.	10.3	186
84	Cu(In,Ga)Se2-based solar cells prepared from Se-containing precursors. Vacuum, 2014, 102, 26-30.	3.5	32
85	Preparation of Cu(In,Ga)Se2 thin film by sputtering from Cu(In,Ga)Se2 quaternary target. Progress in Natural Science: Materials International, 2013, 23, 133-138.	4.4	59
86	Cu2ZnSnSe4 thin film solar cells prepared by rapid thermal annealing of co-electroplated Cu–Zn–Sn precursors. Solar Energy, 2013, 94, 1-7.	6.1	41
87	Preparation and Characterization of Cu(In,Ga)Se ₂ Thin Films by Selenization of Cu _{0.8} Ga _{0.2} and In ₂ Se ₃ Precursor Films. International Journal of Photoenergy, 2012, 2012, 1-7.	2.5	11
88	Study of Cu–In–Ga precursor for Cu(In,Ga)Se2 thin film prepared by the two-stage process. Journal of Materials Research, 2012, 27, 2639-2643.	2.6	4
89	Solution-processed bulk heterojunction solar cells based on interpenetrating CdS nanowires and carbon nanotubes. Nano Research, 2012, 5, 595-604.	10.4	9
90	Double-Walled Carbon Nanotube Solar Cells. Nano Letters, 2007, 7, 2317-2321.	9.1	321

#	Article	IF	CITATIONS
91	Temperatureâ€Gradientâ€Controlled Method Enabling Shape Control of 2D Perovskite Single Crystals for Photodetection. Physica Status Solidi - Rapid Research Letters, 0, , 2100099.	2.4	3
92	The multiple ways of making perovskite/silicon tandem solar cells: Which way to go?. , 0, , .		0
93	Monolithic perovskite/silicon tandem solar cells: combining stability with high performance. , 0, , .		0